(12) INTERNATIONAL APPLICATION PUBLISHED UNDER THE PATENT COOPERATION TREATY (PCT)

(19) World Intellectual Property Organization
International Bureau

(43) International Publication Date
30 January 2003 (30.01.2003)

PCT

(10) International Publication Number
WO 03/007809 A2

(51) International Patent Classification[7]: A61B 5/00

(21) International Application Number: PCT/CA02/01081

(22) International Filing Date: 16 July 2002 (16.07.2002)

(25) Filing Language: English

(26) Publication Language: English

(30) Priority Data:
60/305,092 16 July 2001 (16.07.2001) US
09/985,436 2 November 2001 (02.11.2001) US

(71) Applicant *(for all designated States except US)*: **ART, ADVANCED RESEARCH TECHNOLOGIES INC.** [CA/CA]; 2300 Alfred-Nobel Blvd., Saint-Laurent, Québec H4S 2A4 (CA).

(72) Inventors; and
(75) Inventors/Applicants *(for US only)*: **HALL, David, Jonathan** [GB/CA]; 3445 rue Drummond, app. 1005, Montreal, Québec H3G 1X9 (CA). **KHOL-BAREIS, Mathias** [DE/DE]; Drosselveg 21, 53489 Sinzig (DE).

(74) Agents: **OGILVY Renault** et al.; 1981 McGill College Avenue, Suite 1600, Montreal, Quebec H3A 2Y3 (CA).

(81) Designated States *(national)*: AE, AG, AL, AM, AT, AU, AZ, BA, BB, BG, BR, BY, BZ, CA, CH, CN, CO, CR, CU, CZ, DE, DK, DM, DZ, EC, EE, ES, FI, GB, GD, GE, GH, GM, HR, HU, ID, IL, IN, IS, JP, KE, KG, KP, KR, KZ, LC, LK, LR, LS, LT, LU, LV, MA, MD, MG, MK, MN, MW, MX, MZ, NO, NZ, OM, PH, PL, PT, RO, RU, SD, SE, SG, SI, SK, SL, TJ, TM, TN, TR, TT, TZ, UA, UG, US, UZ, VN, YU, ZA, ZM, ZW.

(84) Designated States *(regional)*: ARIPO patent (GH, GM, KE, LS, MW, MZ, SD, SL, SZ, TZ, UG, ZM, ZW), Eurasian patent (AM, AZ, BY, KG, KZ, MD, RU, TJ, TM), European patent (AT, BE, BG, CH, CY, CZ, DE, DK, EE, ES, FI, FR, GB, GR, IE, IT, LU, MC, NL, PT, SE, SK, TR), OAPI patent (BF, BJ, CF, CG, CI, CM, GA, GN, GQ, GW, ML, MR, NE, SN, TD, TG).

Published:
— *without international search report and to be republished upon receipt of that report*

For two-letter codes and other abbreviations, refer to the "Guidance Notes on Codes and Abbreviations" appearing at the beginning of each regular issue of the PCT Gazette.

(54) Title: CHOICE OF WAVELENGTHS FOR MULTIWAVELENGTH OPTICAL IMAGING

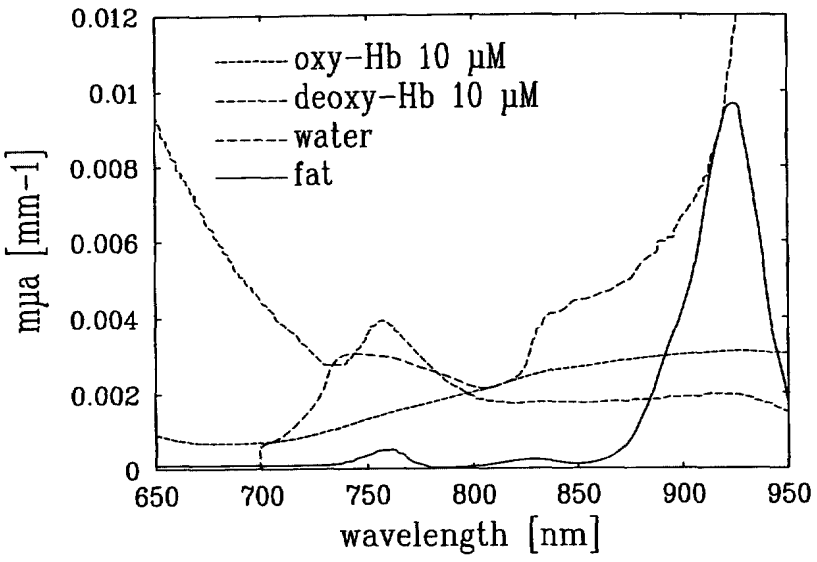

(57) Abstract: The present invention relates to a method for wavelength selection in a multi-wavelength TPSF-based optical imaging system. This consists of identifying several chromophores in a highly turbid medium and selecting optimized wavelengths whereby using these wavelengths optimizes the deduction of the chromophore concentrations. Such chromophore concentrations may be combined to deduce other properties of the turbid medium.

WO 03/007809 A2

CHOICE OF WAVELENGTHS FOR MULTIWAVELENGTH OPTICAL IMAGING

Field of the Invention

The present invention relates to the field of optical imaging in which objects which diffuse light, such as some human body tissues, are imaged using signals resulting from the injection of light into the object and detection of the diffusion of the light in the object at a number of positions. More particularly, the present invention relates to the choice of wavelengths for multiwavelength optical imaging in order to provide enhanced information.

Background of the Invention

Time-domain optical medical images show great promise as a technique for imaging breast tissue, as well as the brain and other body parts. The objective is to analyze the temporal point spread function (TPSF) of an injected pulse as it is diffused in the tissue, and the information extracted from the TPSF is used in constructing a medically useful image.

For example, one can extract time-gated attenuation information from the TPSF which improves the image spatial resolution over previous continuous wave methods. However, it is unclear whether such improvements in image spatial resolution are adequate for diagnosing breast cancer based on morphology.

An alternative approach is to use the TPSF to decouple the light attenuation into absorption and scattering components. This extra information, which cannot be obtained from continuous wave methods, may be clinically useful. Moreover, one can obtain the tissue absorption spectrum by performing time-domain measurements at multiple wavelengths. In tissue there are several molecules which absorb the light and are known as chromophores. Spectroscopic analysis of the tissue absorption spectrum permits chromophore concentrations to be measured. Furthermore, combination of the chromophore concentrations can yield physiological information, as opposed to morphologic information, which could provide a more medically useful image.

The problem is one of knowing which are the dominant chromophores to include in a tissue model and then choosing the "best" wavelengths to deduce their concentrations most accurately.

Summary of the invention

It is an object of the invention to improve image quality in TPSF-based optical images by choosing an efficient combination of wavelengths and combining information from the combination of wavelengths.

It is an object of the present invention to provide an objective method for choosing the wavelengths for a multiwavelength TPSF-based optical imaging approach. For a given set of chromophores, the best selection of the wavelengths is performed for the set as a whole as opposed to choosing the best wavelength for each chromophore individually. Furthermore, hardware constraints can be taken into consideration in order to optimize the selection of wavelengths for a given device.

Brief description of the drawings

Fig. 1 illustrates the absorption spectra used of oxy-Hb, deoxy-Hb, pure water and lipid;

Fig. 2 illustrates the inverse of the condition number of the hemoglobin specific absorption matrix as a function of wavelength $\lambda 1$ being plotted for a system of a) two wavelengths where the other wavelength is fixed at $\lambda 2$ = 850 nm, b) three wavelengths where the other wavelengths are fixed $\lambda 2$ = 850 nm and $\lambda 3$ = 758 nm and c) four wavelengths where the other wavelengths are fixed $\lambda 2$ = 850 nm, $\lambda 3$ = 758 nm and $\lambda 4$ = 800 nm;

Fig. 3 illustrates the inverse of condition number C for the specific absorption spectra of oxy-Hb and deoxy-Hb as a function of $\lambda 1$ and $\lambda 2$. The plot is symmetric with respect to the diagonal. Regions of high values indicate combinations of wavelengths advantageous for spectroscopy;

Fig. 4 illustrates the deviation of calculated saturation and true saturation (S(calc)-S(true)) for a model tissue containing 15 μM [HbT], S(true) = 25%, 50% and 75% and a lipid concentration of 40%. Two wavelengths at 760 and 850 nm were used to fit [oxy-Hb] and [deoxy-Hb]. The sensitivity with respect to wrong assumptions of lipid and water concentrations are shown;

Fig. 5A illustrates the inverse of condition number C for the specific absorption spectra of oxy-Hb and deoxy-Hb and lipid for a fixed wavelength λ = 830 nm as a function of $\lambda 1$ and $\lambda 2$. The islands of high values indicate advantageous wavelengths (scaling 0-0.01);

Fig. 5B illustrates the inverse of condition number C for the specific absorption spectra of oxy-Hb and deoxy-Hb and lipid for a fixed wavelength $\lambda 3$ = 830 nm as a function of $\lambda 1$ and $\lambda 2$ (same as Fig. 5A but scaling 0-0.0005);

Fig. 6A illustrates the inverse of condition number C for the specific absorption spectra of oxy-Hb and deoxy-Hb, lipid and water for two fixed wavelength at $\lambda 3$ = 760 nm and $\lambda 4$ = 830 nm as function of $\lambda 1$ and $\lambda 2$ (scaling 0-0.0015). Regions of high values are advantageous for spectroscopy;

Fig. 6B illustrates the inverse of condition number C for the specific absorption spectra of oxy-Hb and deoxy-Hb, lipid and water for two fixed wavelength at $\lambda 3$ = 760 nm and $\lambda 4$ = 830 nm as function of $\lambda 1$ and $\lambda 2$. (same as Fig. 6A but scaling 0-0.0005);

Fig. 7 illustrates the estimation of deviations from true saturation values for a model tissue of [HbT] = 20 μM, S= 75%, a lipid concentration of 40% and true water concentration corresponding to 0-100% water. Three wavelengths at 760, 780 and 850 nm were used for back calculation of S, shown here as a function of assumed water concentration;

Fig. 8 illustrates the estimation of the influence of errors (noise) in μ_a on the calculated Hb concentrations and saturation values. A model μ_a-spectrum based on 20 μM [HbT], S=50%, and a lipid and water concentration of 30% and 40% was assumed. Matrix inversion was performed for wavelengths 760, 790, 830 and 850 nm. plotted is the change in calculated [oxy-Hb], [deoxy-Hb] and saturation value when the μ_a value at a single wavelength was changed by +0.0001mm^{-1}. This plot suggests that noise at 830 nm translates in the highest noise in saturation values;

Fig. 9 illustrates the estimation of the recovery of saturation values based on different wavelength combinations. A model tissue of 20 μM [HbT], a true saturation of S=75%, lipid and water concentration of 40% were used. in the lower plot an offset of 0.0005 mm^{-1} independent of wavelength was added to the model tissue μa-spectrum (no offset in the upper plot). Plotted are deviations of the saturation values due to matrix inversion and the true 75% value. The following wavelength combinations were used: 1) 760 nm and 850 nm, 2) 760, 830 and 850 nm, 3) 760, 780, 830 and 850 nm, 4) 750-850nm, 5) 720-850 nm, 6) 720-900nm;

Fig. 10 illustrates the estimation of the recovery of saturation values based on different wavelength combinations. A model tissue of 20 μM [HbT], a true

saturation of S=50%, lipid and water concentration of 40% were used. in the lower plot an offset of 0.0005 mm^{-1} independent of wavelength was added to the model tissue μa-spectrum (no offset in the upper plot). Plotted are deviations of the saturation values due to matrix inversion and the true 75% value. The following wavelength combinations were used: 1) 760 nm and 850 nm, 2) 760, 830 and 850 nm, 3) 760, 780, 830 and 850 nm, 4) 750-850nm, 5) 720-850 nm, 6) 720-900nm;

Detailed Description of the invention

In accordance with the present invention, there is provided a method for selecting wavelengths for multiwavelength optical imaging.

Tissue Chromophores

The dominant near infrared chromophores contained in breast tissue are considered to be hemoglobin (Hb) in its oxygenated (oxy-Hb) and deoxygenated (deoxy-Hb) forms, water and lipids. Fig. 1 shows the absorption spectra of oxy-Hb (at 10μM concentration), deoxy-Hb (at 10μM concentration), pure water (100% concentration), lipid (absorption spectrum of olive oil has been used to estimate the absorption spectrum of fat). There are other interesting near infrared chromophores, such as glucose and cytochrome c oxidase, but their absorption contribution in the breast is considered negligible compared to the aforementioned chromophores.

Physiological information

Potentially useful physiological information about the breast tissue can be obtained from concentrations,[], of the chromophores. The total hemoglobin concentration, [HbT], defined as [HbT] = [oxy-Hb] + [deoxy-Hb], is related to the local vascular density. Since cancer is commonly associated with an increase in vascularisation (angiogenesis), a measurement of [HbT] could be medically useful. The fraction of hemoglobin that binds to oxygen is known as the oxygen saturation, S, and defined as S=[oxy-Hb]/[HbT]. Increased metabolic activity increases oxygen demands which decreases the oxygen saturation. Since cancer is commonly associated with increased metabolic activity, a measurement of S could also be medically useful.

Wavelength Choice

Historically as the biomedical optics field evolved the wavelengths were chosen for each chromophore individually by observing strong near infrared spectral

features for the given chromophore and using the closest hardware-available wavelength. Many researchers also used the isobestic wavelength of oxy-Hb and deoxy-Hb, the wavelength where their absorption per concentration are equal, since this wavelength is insensitive to the oxygenation state of the hemoglobin and can be related to the [HbT].

However, the question both posed and addressed here is that for a given set of chromophores what are the optimal wavelengths to use in order to deduce the concentration of each chromophore? It is interesting to note that the isobestic wavelength used by many researchers turns out not to be one of the wavelengths of choice.

It is an object of the present invention to provide an objective method for choosing the wavelengths for a multiwavelength TPSF-based optical imaging approach. For a given set of chromophores, the best selection of the wavelengths is performed for the set as a whole as opposed to choosing the best wavelength for each chromophore individually. Moreover, it is also possible to investigate scenarios such as the influence on determining chromophore concentrations under certain assumptions about the concentration(s) of other chromophore(s) in the set. Furthermore, hardware constraints can also be taken into consideration in order to optimize the selection of wavelengths for a given device. Fortunately, the recent advent of turn-key, pulsed, tunable near infrared wavelength lasers has permitted more viable availability of near infrared wavelengths.

Experimental brute force approach

One possible approach to optimize the choice of wavelengths for a given set of chromophores is to conduct a brute force experimental study. This would consist of performing numerous experiments where different combinations of wavelengths are evaluated for the given set of chromophores at known concentrations until the optimum combination for deducing their concentrations is found. Obviously, this approach is likely to be highly time-consuming and it is not always trivial to provide a set of chromophores at known concentrations, particularly in the case of in vivo breast tissue.

Matrix inversion sensitivity approach

An alternative approach which avoids the numerous experiments of the experimental brute force approach is a matrix inversion sensitivity approach.

The equation which needs to be solved can be written for each wavelength as:

$$\mu_a(\lambda_1) = \sum_i m_{a,i}(\lambda_1) \cdot c_i$$

$$\mu_a(\lambda_2) = \sum_i m_{a,i}(\lambda_2) \cdot c_i$$

.....

$$\mu_a(\lambda_3) = \sum_i m_{a,i}(\lambda_3) \cdot c_i$$

where μ_a is the measured absorption coefficient, m_a is the specific absorption coefficient of the different chromophores and c_i is the corresponding concentration.

This is written is matrix form as:

$$\boldsymbol{\mu_a = M \cdot c}$$

where printing in bold indicates a matrix or vector. $\boldsymbol{\mu_a}$ is a vector with a number of rows corresponding to the number of wavelengths (n_λ). **c** is a vector with the number of rows corresponding to the number of chromophores (n_c). **M** is a rectangular matrix of size n_λ x n_c.

If $n_\lambda = n_c$ the system can be solved by matrix inversion $\mathbf{c=M^{-1}\mu_a}$ and if $n_\lambda > n_c$ the system is overdetermined and can be solved by the pseudo-inverse $\mathbf{M^+} = (\mathbf{M^T M})^{-1} \mathbf{M^T}$ where $\mathbf{M^T}$ is the transposed matrix of **M**.

$$\mathbf{c} = (\mathbf{M^+})\boldsymbol{\mu_a}$$

The pseudoinverse $\mathbf{M^+}$ is an n_λ x n_c array which is unique. If **M** is square (i.e. not overdetermined) the $\mathbf{M^+} = \mathbf{M^{-1}}$. For given (i.e. chosen) wavelengths the pseudoinverse $\mathbf{M^+}$ can be precalculated once and the matrix inversion corresponds to a simple matrix multiplication. This is the basis for the calculation of chromophore concentration.

One means to quantify the expected sensitivity of a matrix inversion of a matrix **M** with respect to small errors in the data is the condition number C which is defined as:

$$C = \text{norm}(\mathbf{M}) \cdot \text{norm}(\mathbf{M^{-1}})$$

C gives an indication of the accuracy of the results and is an estimate of the cross-talk between the different channels (i.e. chromophores concentrations).

Values of C near 1 indicate a well-conditioned matrix, large values indicate an ill-conditioned matrix. The condition number is closely related to singular value decomposition (SVD) as it is the ratio of the largest and the smallest singular value of a matrix.

The matrix M for oxy-Hb and deoxy-HB at λ = 760 and 770 nm is

$$M = \begin{matrix} 0.3871 & 0.1465 \quad \lambda = 760nm \\ 0.3280 & 0.1625 \quad \lambda = 770nm \end{matrix}$$

A matrix inversion is possible as the rank (**M**) = 2, however the absorption at the two wavelengths is 'similar'. The condition number is C = 20.49. Choosing the wavelengths to be λ = 760 and 850 nm gives the matrix

$$M = \begin{matrix} 0.3871 & 0.1465 \\ 0.1729 & 0.2645 \end{matrix}$$

Inspection by eye already shows that the absorption is very 'different'. This is confirmed by the condition number: C=3.206. In what follows below the inverse of the condition number is plotted and analyzed. It has value between 0 and 1. 1/C close to 1 means 'orthogonal' spectra and low sensitivity to cross-talk. Small values of 1/C mean an ill-conditioned matrix. To find the best wavelengths, 1/C is calculated as a function of a wavelength. The wavelengths that give the highest values of 1/C are the best for a calculation of chromophore concentrations and the subsequent physiological information such as oxygen saturation, S.

Model absorption spectra were generated with the absorption spectra of Fig. 1 based on estimations of [HbT], S, lipid and water concentration. Matrix inversion based on different sets of wavelengths were performed to recover these parameters. These parameters were compared with the true ones for the different wavelengths and the sensitivity to noise or measurement offsets considered.

Assuming that we fit for the hemoglobin concentrations only and assuming certain values for water and lipid concentration, for a x-wavelengths matrix inversion, the best combination of wavelengths to give a well-conditioned matrix, the sensitivity of calculated values of oxy-Hb and deoxy-Hb concentration and oxygen saturation for variations of lipid or water concentration and sensitivity of S to measurement noise have been determined.

In Fig. 2 the inverse of the condition number is shown for matrices of oxy-Hb and deoxy-Hb specific absorption coefficients for 2, 3 and 4 wavelengths. In each case one wavelength (λ_1) was varied between 650 and 950 nm while the remaining wavelengths were fixed λ_2 = 850 nm (2-wavelength system), λ_2 = 850 nm and λ_3 = 758 nm (3-wavelength system), and λ_2 = 850 nm, λ_3 = 758 nm and λ_4 = 800 nm (4-wavelength system). Fig. 2 indicates that the selection of two wavelength at λ_1 = 850 nm and λ_2 = 700 nm gives the highest values of 1/C and when the wavelength range is restricted via hardware constraints to > 750 nm, a system that includes the peak wavelength of deoxy-Hb close to 760 nm is advantageous. It does not matter whether two or more wavelengths are used. This somewhat counterintuitive result is valid only without measurement noise and noise in the background absorption.

Fig. 3 further highlights this finding for a two-wavelength matrix inversion. In this figure 1/C is plotted as a function of both at λ_1 and λ_2 in the range 650-950 nm. The plot is symmetric with respect to the diagonal. Regions of high 1/C-values can be chosen and the corresponding 'good' wavelengths can be read off the axis. It is apparent that (with the restriction to > 750 nm) the one wavelength should be close to 760 nm while the other one can be within the range 830-900 nm without substantially affecting the condition number.

Using the spectra shown in Fig.1, model tissue absorption spectra were generated. Based on matrix inversion values of [oxy-Hb], [deoxy-Hb] and S were backcalculated and the sensitivity to incorrect assumptions about the [water] and [lipid] tested. One approach is to take the measured μ_a spectra and subtract water and lipid absorption corresponding to certain assumed concentrations. For the data shown in Fig. 4, a model tissue containing 15 μM [HbT], (true) saturation values of S = 25%, 50% and 75% was used. Lipid concentration was 40%. It was tested how a misjudgement of water concentration affects the recalculated S value. To test the error in a simple two-wavelengths-fit (760 and 850 nm), the assumed lipid concentration was varied between 0 and 100%. When the assumed water concentration is right (lower three lines in Fig. 4), the deviation in saturation between true and calculated values is < ±2% (obviously with zero error for the right lipid concentration of 40%). A misjudgement about the water concentration by 20% (upper lines in Fig. 5) results in additional errors in S(calc)-S(true) of up to 2% for S=75%, 4% for S=50% and 8% for S=25%. These errors in S are a function of the underlying tissue absorption coefficients. The values here give an indication about the order of magnitude.

Having a system with more than two fit-parameters, best wavelength combinations, for a three-components system of oxy-Hb, deoxy-Hb and lipid system, for a four-components system of oxy-Hb, deoxy-Hb, lipid and water, and the sensitivity of calculation of S to noise at the different wavelengths have been determined.

In Figs. 5A and 5B the inverse of the condition number is plotted for a three wavelengths system based on the oxy-Hb, deoxy-Hb and lipid specific absorption spectra as a function of λ_1 and λ_2. The third wavelength was fixed at $\lambda 3$ = 830 nm. Again, the plot is symmetric with respect to the diagonal. From Fig. 5A it is apparent, that there are three "islands" of high 1/C values. Unfortunately, all of these island would include wavelengths outside an imposed hardware constrained wavelength range of 750 to 850 nm. Plotting the same data in a different scale (Fig. 5B) shows that there is just a single preferential combination within this hardware constrained wavelength range: 760 and 780 nm.

Equivalent to Figs. 5A and 5B, the inverse of C for a 4-wavelengths system is plotted in Fig. 6A and 6B. Again, the difference between them is the scaling. Two wavelengths were fixed at $\lambda 3$ = 760 nm and $\lambda 4$ = 830 nm. Including the wavelengths outside the 750-850 nm range there appear four preferential combinations. Restricting the wavelength range to 750-850 nm there are just two advantageous region (marked by the white rectangle in Fig. 6B): 780 nm and 850 nm, and 780 nm and 815 nm.

From the analysis based on matrix condition numbers, the best wavelength combinations for 2, 3 and 4 wavelengths measurements are the following:

Table 1

Wavelength combinations for 2, 3 and 4 wavelengths measurements

	Wavelength Range	Best wavelengths (nm) λ1	λ2	λ3	λ4	fit for	see Fig.
2-λ	650-950 nm	700	>860			Oxy-Hb, deoxy-Hb	2,3
	750-850 nm	760	850				
3-λ	650-950 nm	700-760	830	925		+ lipid	5 A,B
		830	860-870	925			
	750-850 nm	760	780	830			
4-λ	650-950 nm	760	830	860	925	+ lipid, + water	6A,B
		700	760	830	925		
	750-850 nm	760	780	830	850	**Best combination**	
		760	780	815	830		

Furthermore, it must be pointed out that including more wavelengths does not increase the condition number. E.g. for the four chromophores and all wavelengths in the range 750-850 nm, 1/C = 0.000314. This is lower than the value (1/C = 0.00036, compare with Fig. 6B) when only four wavelengths (760, 780, 830 and 850 nm) are used. In a system without noise and no other chromophores than the four considered here, a 4-wavelengths system is the optimal.

While certainly only a 4-wavelengths measurement allows [oxy-Hb], [deoxy-Hb], [lipid] and [water] to be determined, and a 2-wavelengths system (see Fig. 5) is not sufficient, the question is posed whether a 3-wavelengths measurement might supply S values with a high enough precision. In this case the concentration of one chromophore (water or lipid) must be guessed and the corresponding absorption subtracted from the measured μ_a values. This was tested with a model absorption spectrum and is shown in Fig. 7 for 760, 780 and 850 nm. True water concentration was varied between 10 and 100% (the different lines), and the difference between calculated and true saturation values plotted as a function of assumed water concentration. For instance, for a true

water concentration of 50%, a misjudgment of the water concentration by 10% results in an error in S by about 4%.

Up to now, only "perfect" data sets were considered with no noise. In real situations there are problems due to measurement noise that is random for the different wavelengths; unknown chromophores in the tissue, i.e. there is a background absorption coefficient the spectrum of which we do not know; and possible systematic errors in the primary μ_a recovery.

There are an ample number of parameters which can be considered and as examples the following two questions are considered. First, is the oxygen saturation more susceptible to noise at certain wavelengths? Second, what is the influence of an offset in the μ_a data?

The influence of errors (noise) in μ_a on the calculated Hb concentrations and saturation values was estimated in a model tissue based on 20μM [HbT], S= 50% and a lipid and water concentration of 30% and 40% respectively. Matrix inversion was performed on the μ_a - spectrum of this model tissue for wavelengths 760, 780, 830 and 850 nm. The sensitivity to noise (i.e. variations in μa) at the different wavelengths was estimated by changing the absorption coefficient at a single wavelength by +0.0001 mm^{-1}. In Fig. 8, the change in calculated [oxy-Hb], [deoxy-Hb] and oxygen saturation value due to this "noise" is plotted. This figure shows that the change in oxygen saturation value is about -2% for changes at 760 nm, <0.5% at 780nm, while it translates to a variation of +6% at 830 nm.

There are two conditions that produce an offset in the measured μa-spectra with respect to the true values. First, the algorithm for μ_a-calculation based on TPSF-based optical imaging might lead to a systematic offset e.g. due to residual crosstalk between absorption and scattering parameters. Second, the tissue absorption might have a background of unknown origin (chromophore). Under both conditions the fitting of μ_a-data with the four chromophores is hampered. The effect of such an offset for different wavelength combinations is estimated with a model spectrum of 20 μM [HbT], S=75% and water and lipid concentration of 40%. An offset of 0.0005 mm^{-1} was added to the μ_a-values independent of wavelength. The effect on the calculated oxygen saturation values is known in Fig. 9 for combination of 2, 3 and 4 wavelengths as well as continuous spectra between 750-850, 720-850 and 720-900 nm. It is apparent that the lowest error in S is achieved by the 4-wavelengths combination. Including more wavelengths

increases the error. In Fig. 10 the same calculation was done, however, for a true oxygen saturation value of 50%. Here the lowest error is achieved by the 720-850 nm wavelength range, while using less wavelengths or increasing the fitting range to 900 nm results in larger errors.

Based on the assumption that the dominant tissue chromophores are oxy-Hb, deoxy-Hb, water and lipid and analysis of the matrix condition number, measurements at the wavelengths 760, 780, 830 and 850 nm supply an optimal data set when the wavelength range is limited to 750-850 nm under ideal conditions. As shown in Figs. 5 and 6, inclusion of shorter and longer wavelengths promise a better matrix inversion. Under real conditions there is no clear-cut answer about the improvement when more wavelengths are included (see Figs. 9 and 10). It might be advantageous to reduce measurement noise at 4 wavelengths due to longer scan times rather than to include more wavelengths. As demonstrated in Fig. 8, to achieve an optimal accuracy the noise level at different wavelengths has to be adjusted which might require different measurement times at certain wavelengths.

Strictly speaking the work presented here was achieved by optimizing a 2-wavelength system and then optimizing a 4-wavelength system where 2 of the wavelengths were fixed at the optimized 2-wavelength system values. Whilst this is easier to display graphically, preferably all 4 wavelengths would be permitted to vary in a global optimization process. Fortunately, for the specific example presented here when all 4 wavelengths are permitted to vary the same optimal solution is found. However, this may not be true for all situations and a global optimization is preferred.

It is also understood that it will be obvious to those skilled in the art that the same approach for choosing optimal wavelengths can be applied to optical absorption spectroscopy in general. For example, in other embodiments of the present invention the method of the present invention is also used for choosing the optimal wavelengths for analyzing the components of paints, pharmaceutical products, food, grain or any other turbid media.

It is also understood that the proposed method applies both to the analysis of absolute chromophore concentrations as to their changes or relative concentrations.

While the invention has been described in connection with specific embodiments thereof, it will be understood that it is capable of further modifications and this

application is intended to cover any variations, uses, or adaptations of the invention following, in general, the principles of the invention and including such departures from the present disclosures as come within known or customary practice within the art to which the invention pertains and as may be applied to the essential features herein before set forth, and as follows in the scope of the appended claims.

CLAIMS

1. A method of optical imaging of turbid media using a plurality of discrete wavelengths in an optical imaging system, the method comprising the steps of:

selecting a set of chromophores for characterizing a property of the turbid media;

defining parameters of the system including at least a number of said discrete wavelengths, a value of each of said wavelengths, source power and detector aperture for each of said wavelengths, a choice of image algorithm and source/detector geometries, a choice of source and detector and noise characteristics;

fixing a value of all of said parameters except a plurality of said parameters values to be optimized;

determining an optimal value for each of said parameter values to be optimized as a function of a performance of the system in measuring a concentration of said chromophores in said turbid media for characterizing said property as a whole; and

using said optimal value for each of said parameter values in imaging said turbid media.

2. The method of claim 1, wherein said imaging is medical imaging, said highly turbid medium being body tissue and said property is physiological.

3. The method of claim 1 or 2, wherein said parameter values to be optimized comprise a value of each of said wavelengths.

4. The method of claim 3, wherein said parameter values to be optimized further comprise said number of said discrete wavelengths.

5. The method of claim 4, wherein said step of determining comprises fixing said number of discrete wavelengths at each of a plurality of numbers, and

determining an optimized performance of the system in measuring a concentration of said chromophores in said turbid media at each of said plurality of wavelengths, and selecting one of said plurality of numbers having a best optimized performance.

6. The method of claim 3, wherein said step of determining an optimal value for each of said parameters comprising minimizing a condition number of a matrix of specific absorption coefficients of said chromophores as a function of wavelength.

7. The method of claim 4, wherein said step of determining an optimal value for each of said parameters comprises minimizing a condition number of a matrix of specific absorption coefficients of said chromophores as a function of wavelength.

8. The method of claim 5, wherein said step of determining an optimal value for each of said parameters comprises minimizing a condition number of a matrix of specific absorption coefficients of said chromophores as a function of wavelength.

9. The method of claim 1, wherein said step of determining comprises empirically determining said performance of the system for a range of said values for each of said parameter values to be optimized.

10. The method of claim 2, wherein said plurality of chromophores comprise at least oxy-hemoglobin and deoxy-hemoglobin.

11. The method of claim 10, wherein said chromophores are water, lipids, oxy-hemoglobin and deoxy-hemoglobin.

12. The method of claim 10, wherein said body tissue is breast tissue.

13. The method of claim 10, wherein said number of wavelengths selected is from 2 to 4.

14. The method of claim 13, wherein said number is 4.

15. The method of claim 11, wherein values of said wavelengths are 760 nm, 780 nm, 830 nm and 850 nm.

16. The method of claim 1, wherein the step of determining an optimal value of said parameters to be optimized comprises:

deriving an inherent wavelength-dependent sensitivity to noise in calculating said chromophore concentrations, and

determining an optimal correlation of said sensitivity and at least one other of said parameters.

17. The method of claim 16, wherein one of said parameters to be optimized is a distribution of an acquisition time at each of said wavelengths.

18. The method of claim 1, wherein one of said parameters to be optimized is a distribution of an acquisition time at each of said wavelengths.

19. The method of claim 18, further comprising a step of determining a minimum value for said acquisition time at which said performance of said system attains a minimum threshold value.

20. The method of claim 1, wherein one of said parameters to be optimized is at least one of said source power and said detector aperture for each of said wavelengths.

21. The method of claim 20, further comprising a step of determining a minimum value for an acquisition time at which said performance of said system attains a minimum threshold value.

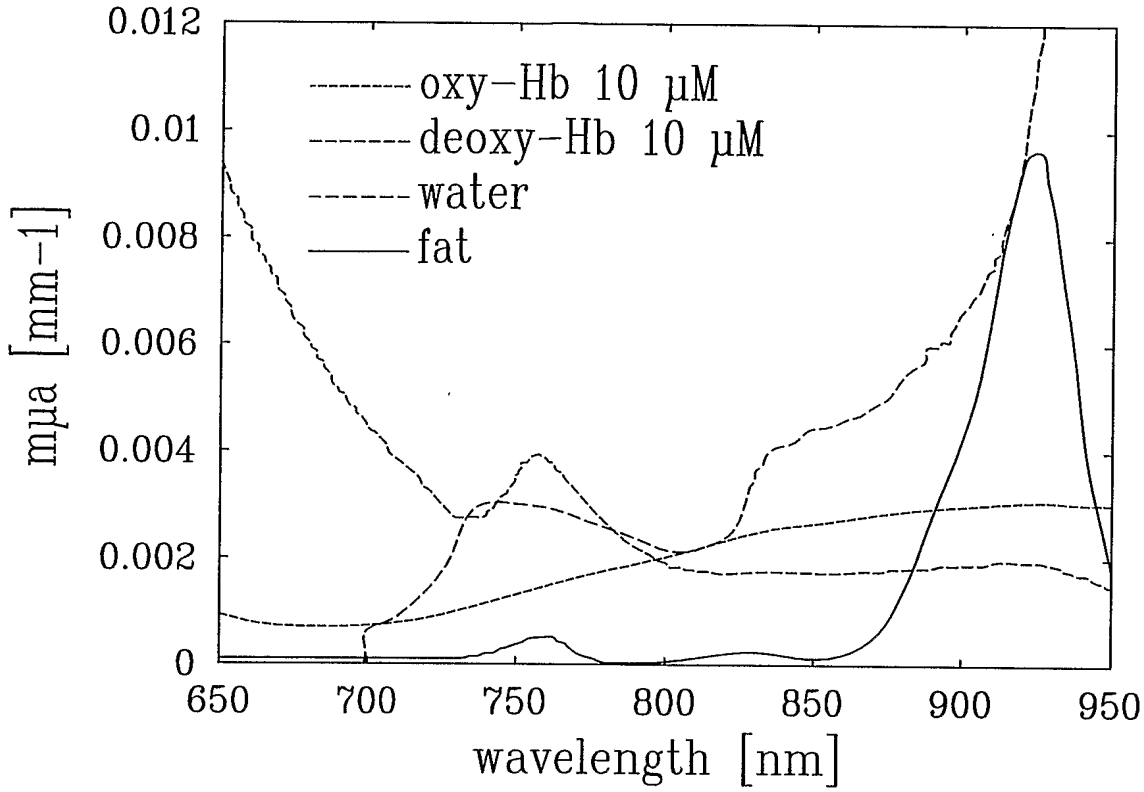
0.012
0.01
0.008
0.006
0.004
0.002
0
mμa [mm-1]
oxy-Hb 10 μM
deoxy-Hb 10 μM
water
fat
650
700
750
800
850
900
950
wavelength [nm]

Fig_1

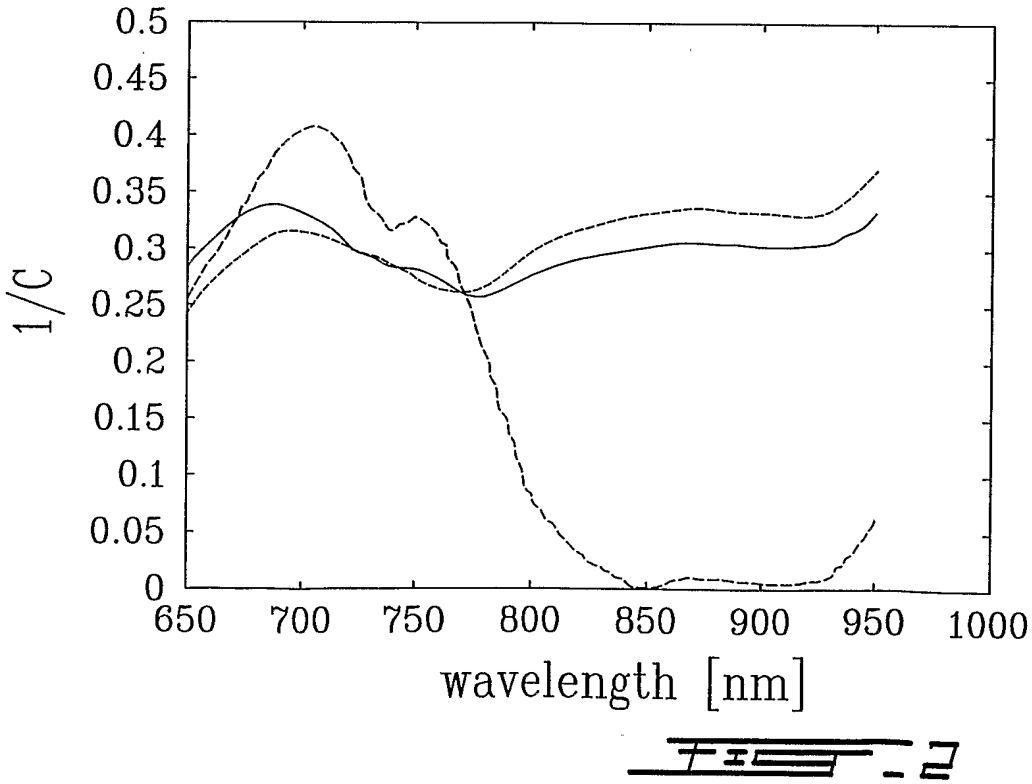
0.5
0.45
0.4
0.35
0.3
0.25
0.2
0.15
0.1
0.05
0
1/C
650
700
750
800
850
900
950
1000
wavelength [nm]

Fig_2

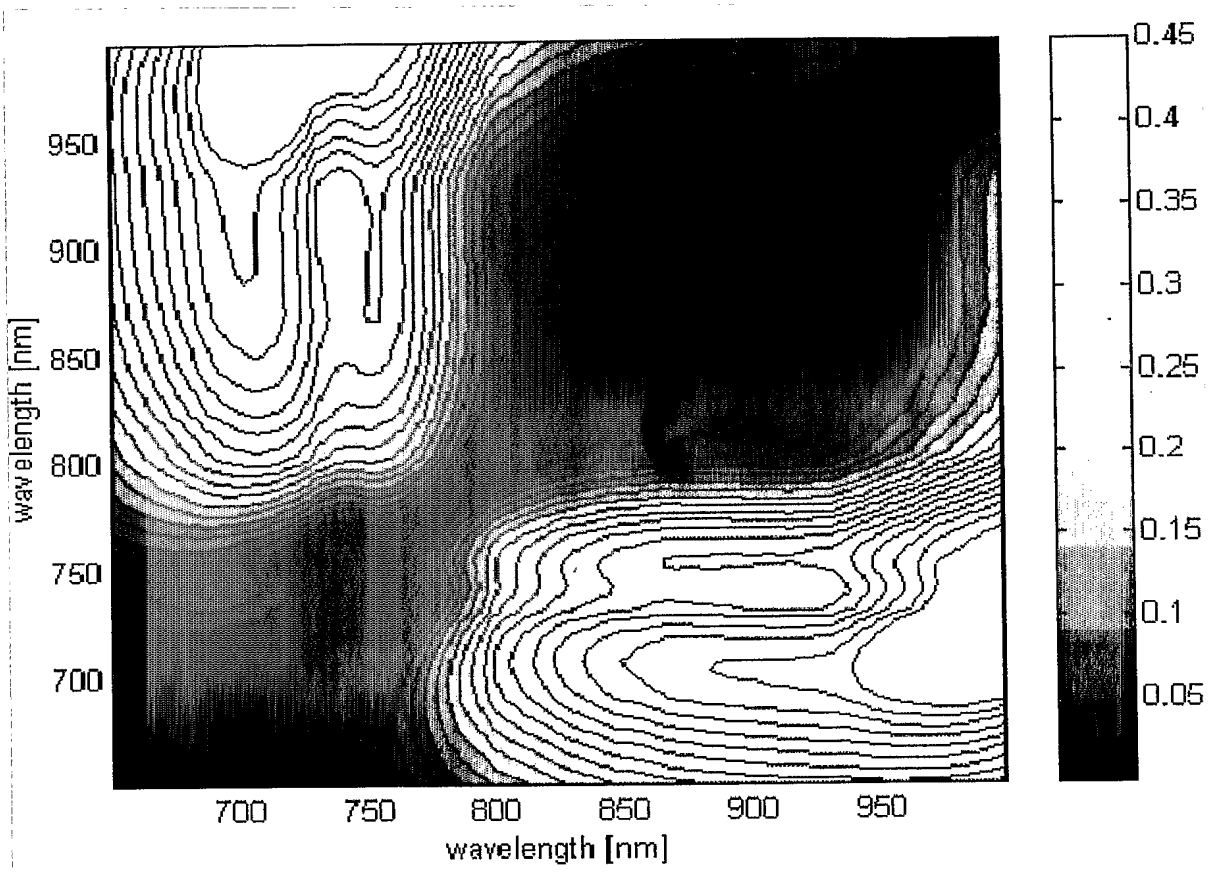
950
900
850
800
750
700
wavelength [nm]
700
750
800
850
900
950
wavelength [nm]
0.45
0.4
0.35
0.3
0.25
0.2
0.15
0.1
0.05

Fig. 3

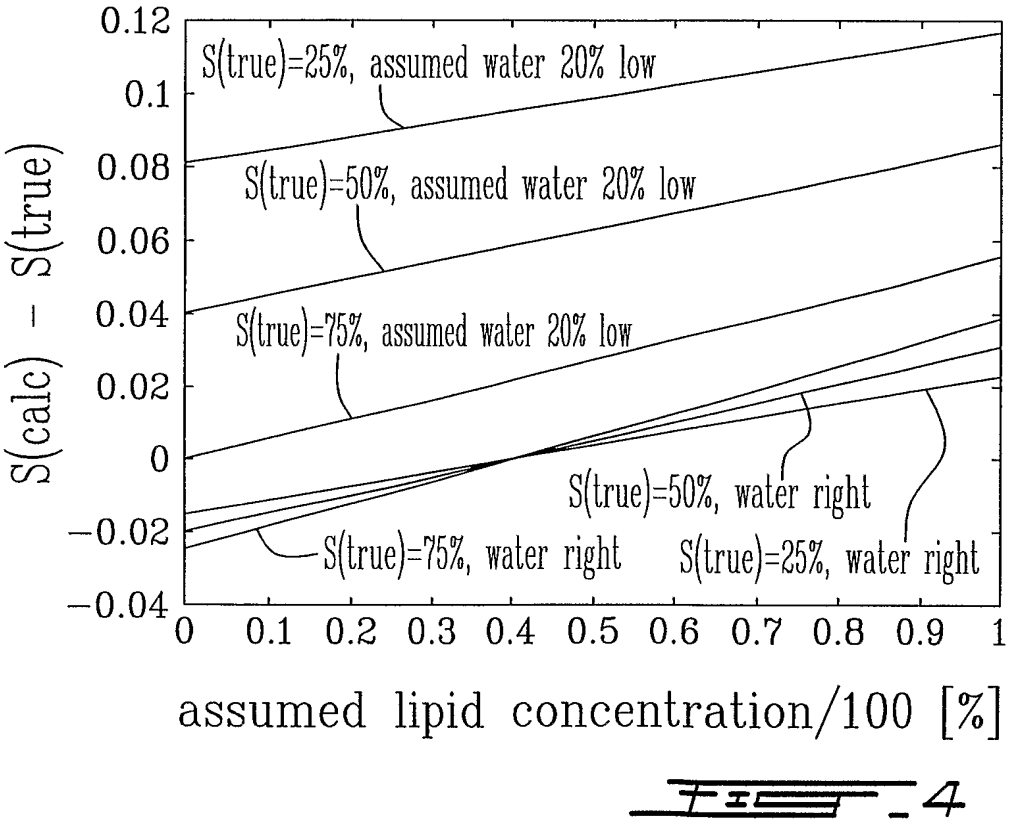
0.12
0.1
0.08
0.06
0.04
0.02
0
−0.02
−0.04
S(calc) − S(true)
S(true)=25%, assumed water 20% low
S(true)=50%, assumed water 20% low
S(true)=75%, assumed water 20% low
S(true)=50%, water right
S(true)=75%, water right
S(true)=25%, water right
0 0.1 0.2 0.3 0.4 0.5 0.6 0.7 0.8 0.9 1
assumed lipid concentration/100 [%]

Fig. 4

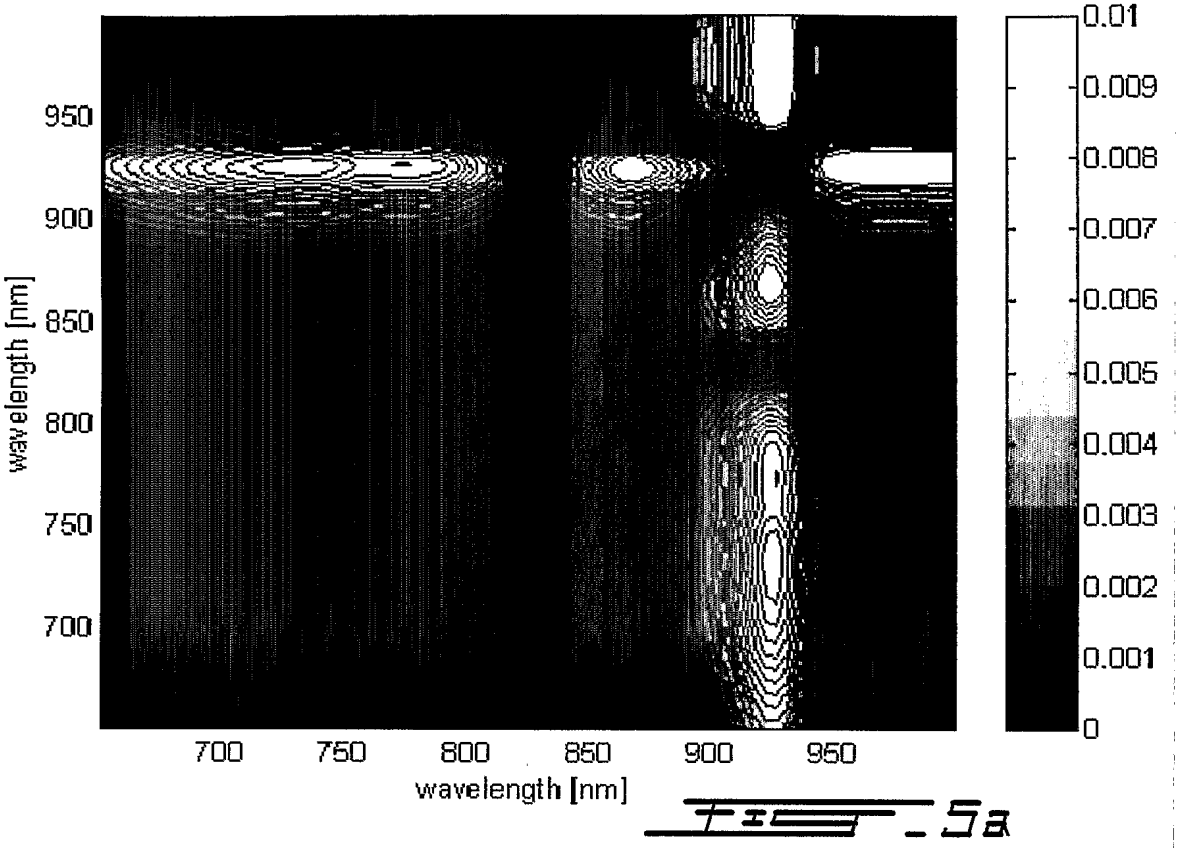
wavelength [nm]
700
750
800
850
900
950
wavelength [nm]
0.01
0.009
0.008
0.007
0.006
0.005
0.004
0.003
0.002
0.001
0

Fig. 5a

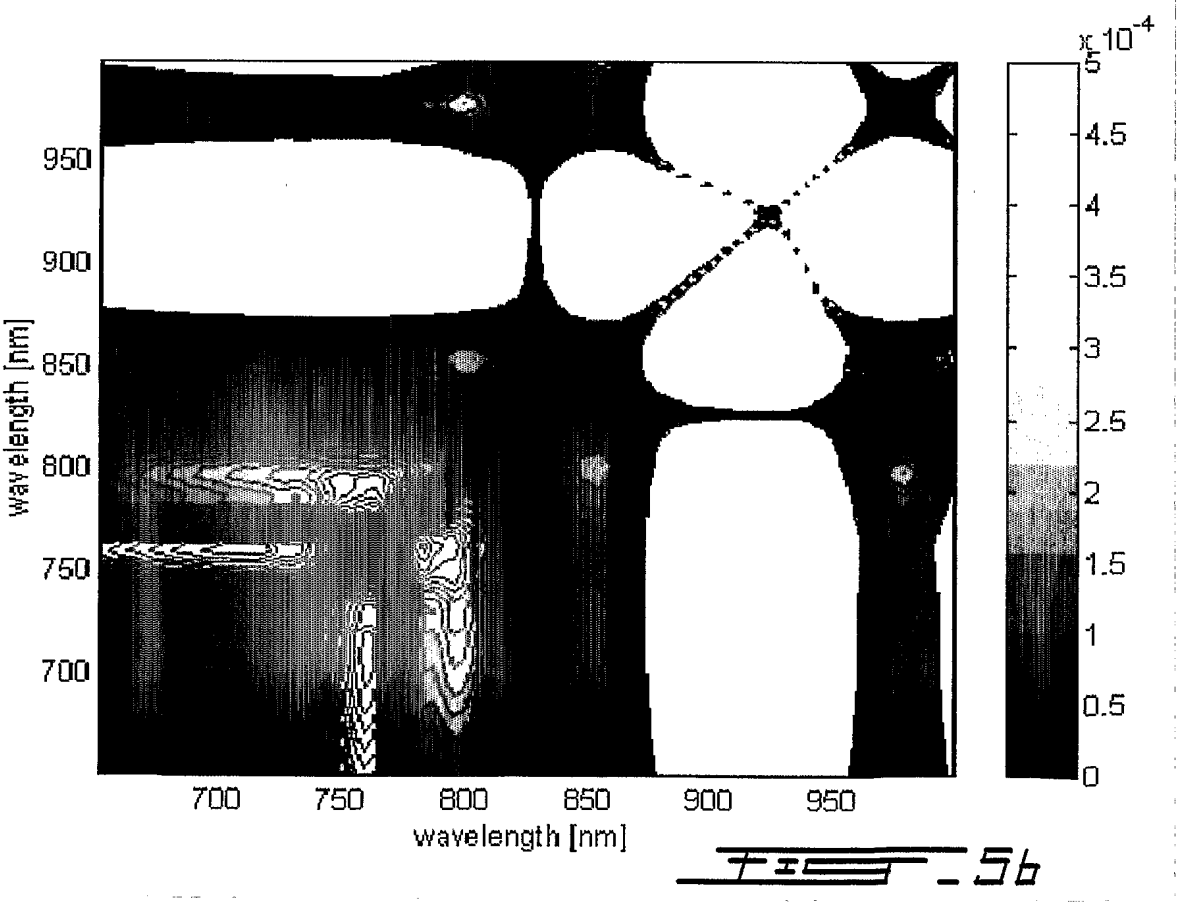
wavelength [nm]
700
750
800
850
900
950
wavelength [nm]
x 10^-4
5
4.5
4
3.5
3
2.5
2
1.5
1
0.5
0

Fig. 5b

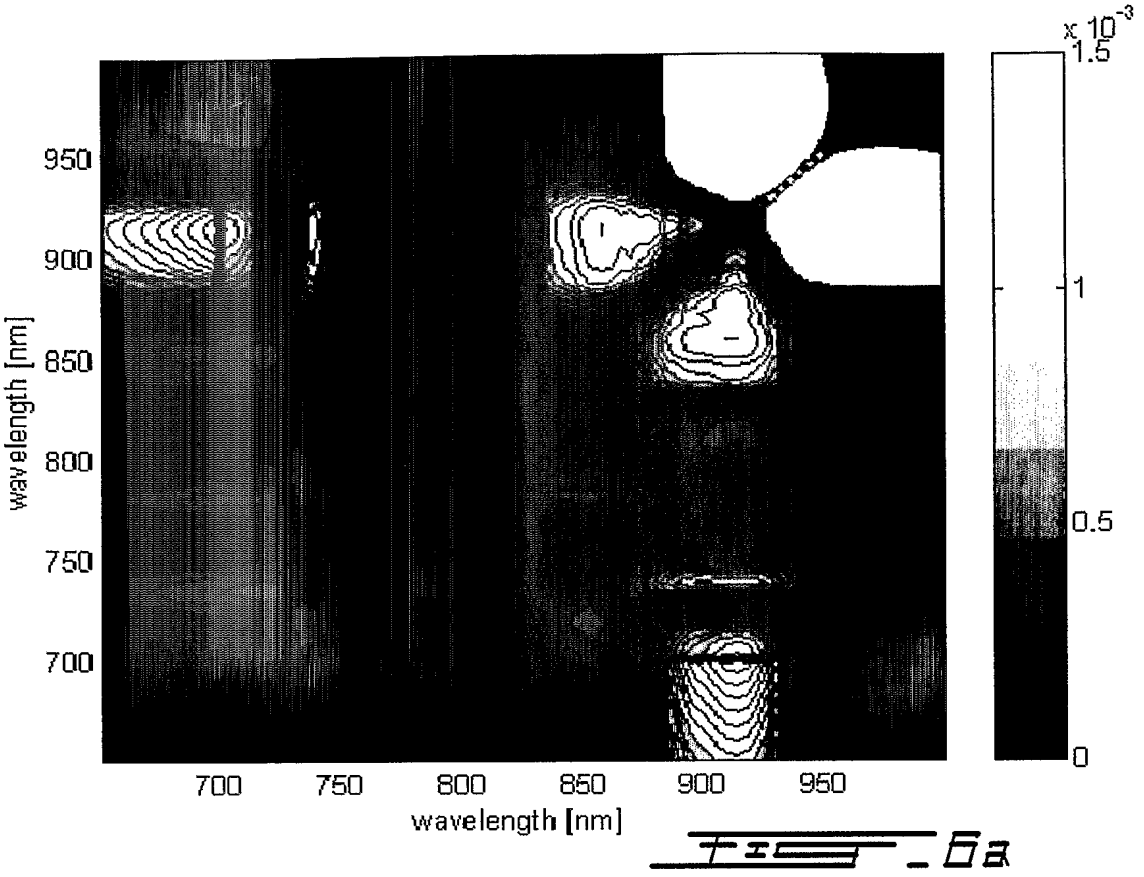
x 10^-3
1.5
1
0.5
0
950
900
850
800
750
700
wavelength [nm]
700
750
800
850
900
950
wavelength [nm]

Fig. 6a

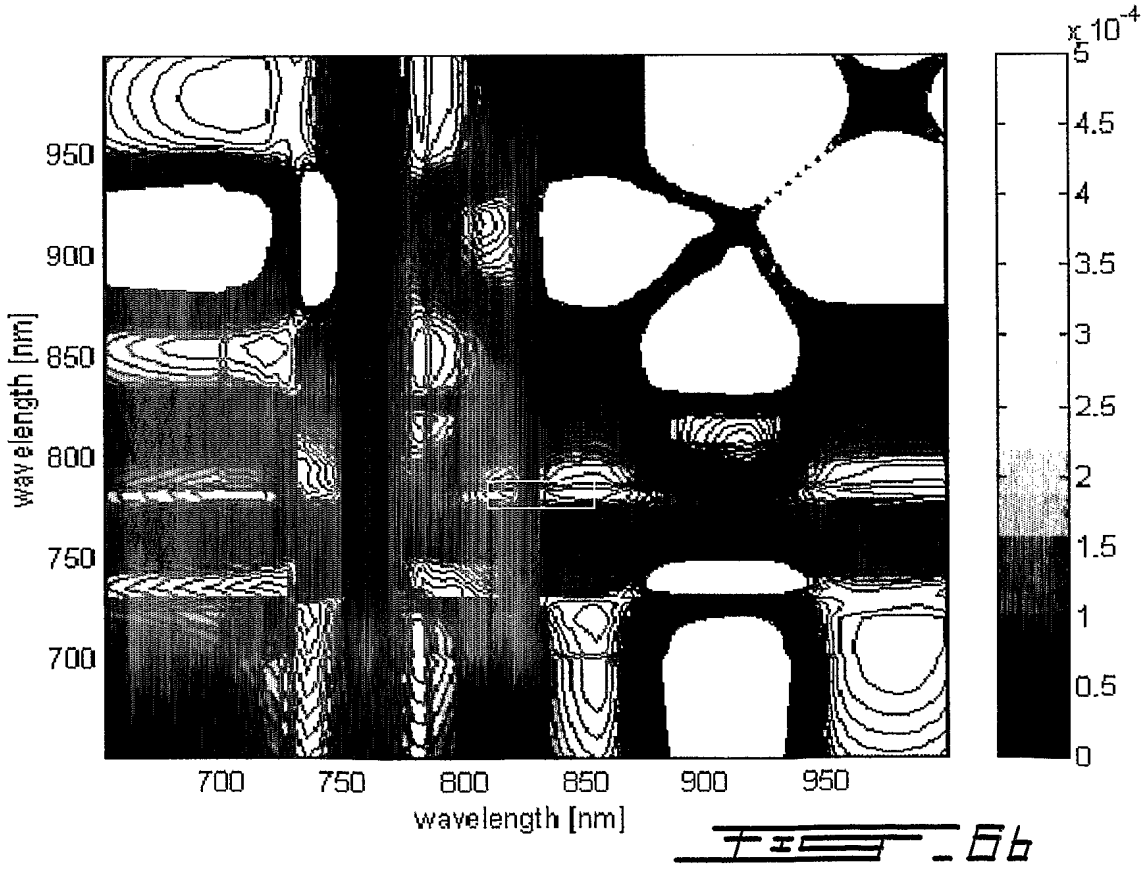
x 10^-4
5
4.5
4
3.5
3
2.5
2
1.5
1
0.5
0
950
900
850
800
750
700
wavelength [nm]
700
750
800
850
900
950
wavelength [nm]

Fig. 6b

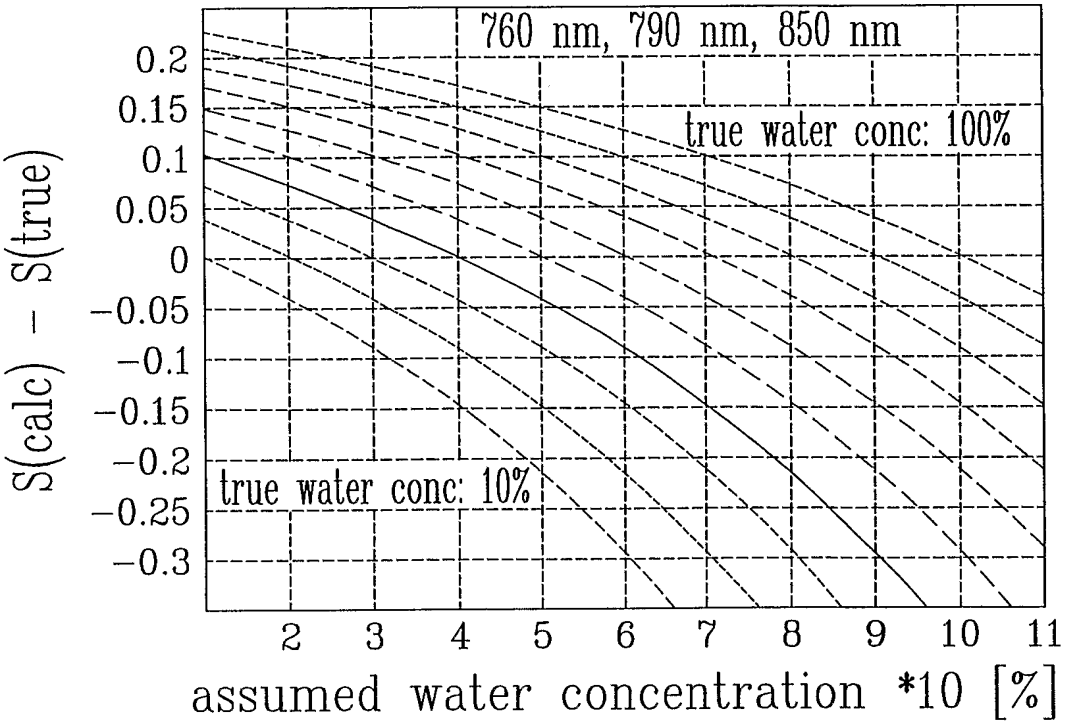

Fig. 7

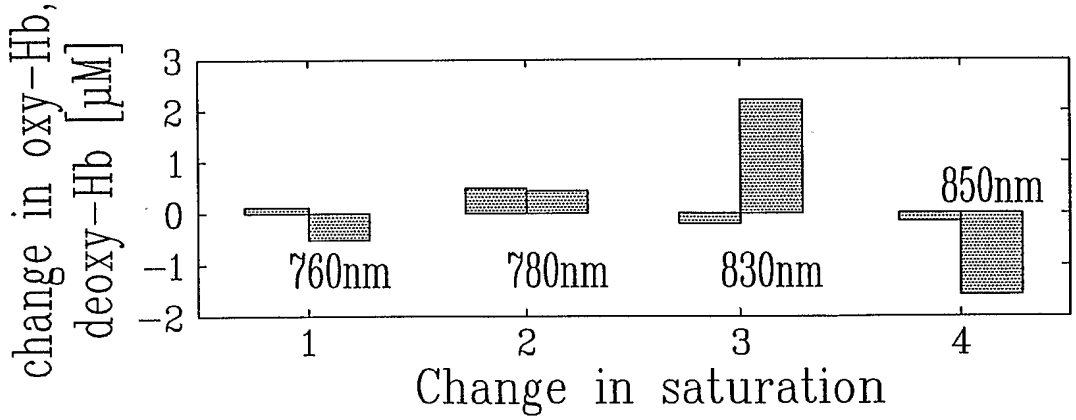

Fig. 8A

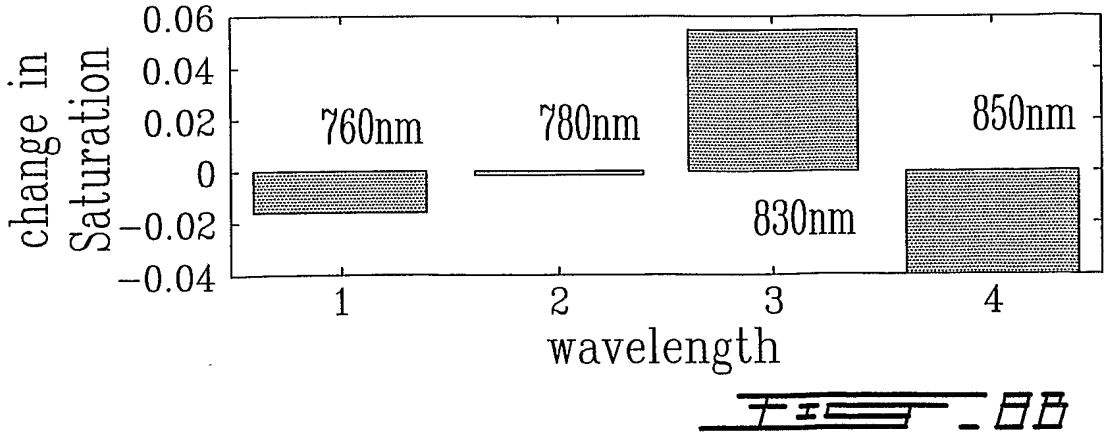

Fig. 8B

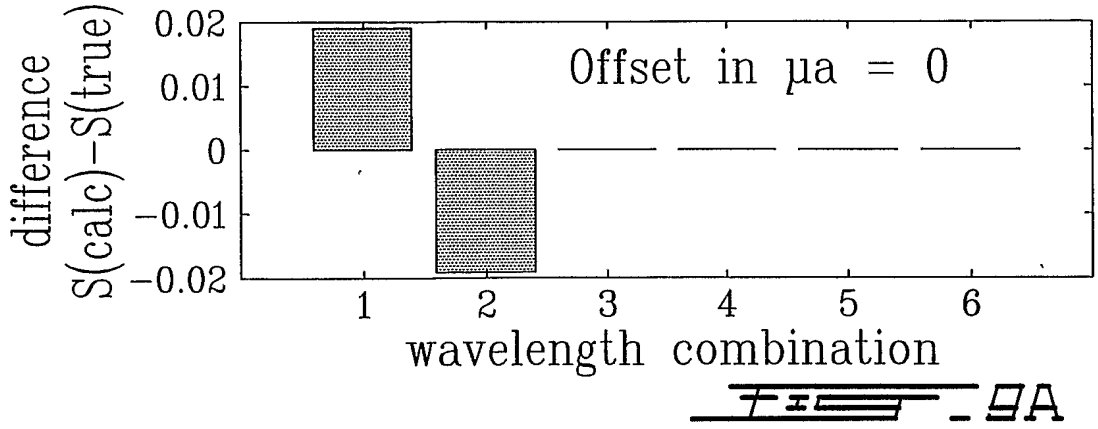

Fig 9A

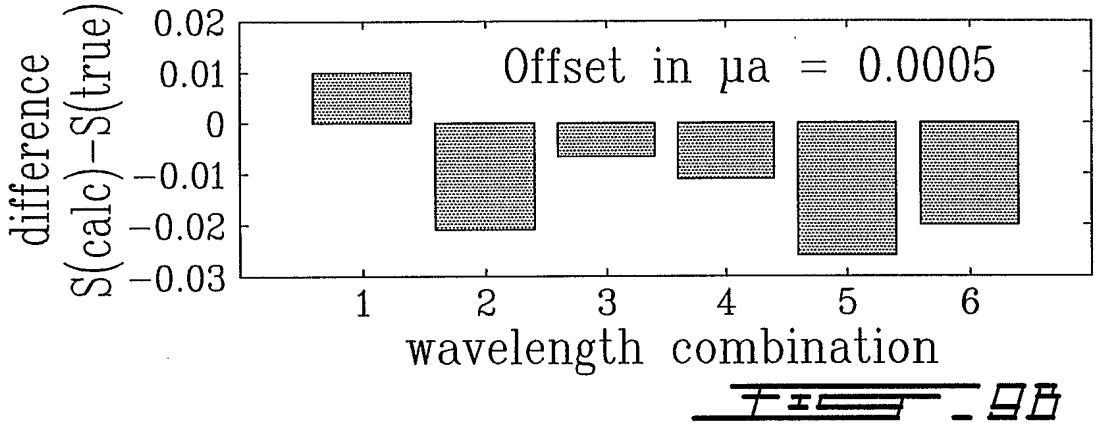

Fig 9B

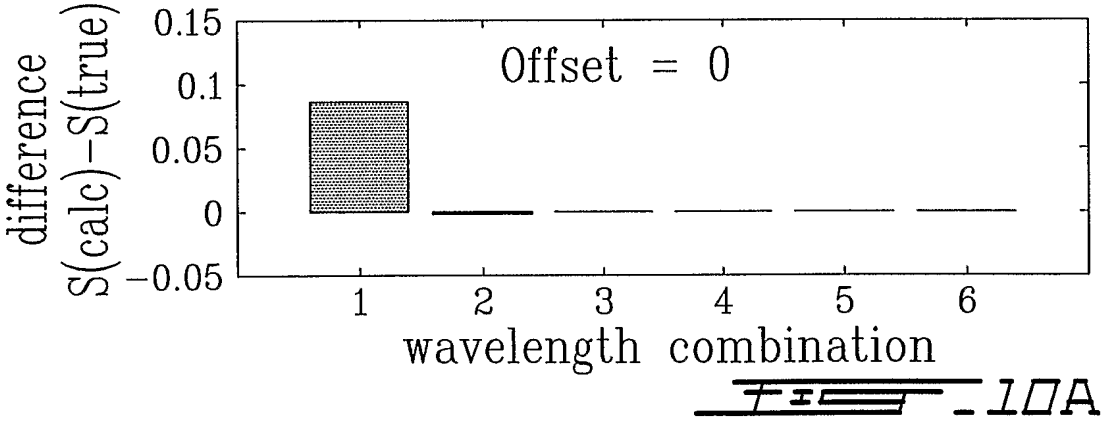

Fig 10A

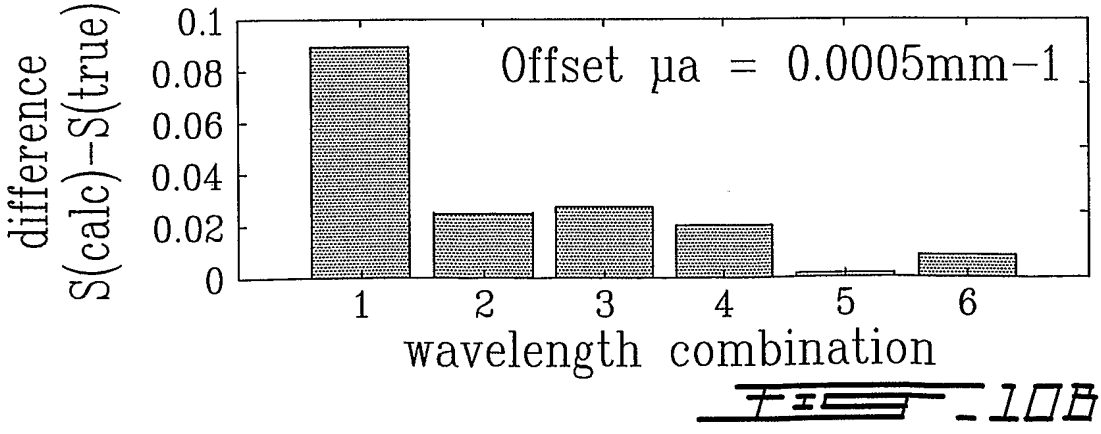

Fig 10B